ERJ Express. Published on April 8, 2009 as doi: 10.1183/09031936.00171808

Growth hormone excess and sternohyoid muscle mechanics in rats

P. Attal,[2] V. Claes,[4] S. Bobin,[2] P. Chanson,[3,6] P. Kamenicky, [3,6] P. Zizzari, [7] and Y. Lecarpentier,[1,5]

Services de [1]Physiologie, d'[2]Oto-rhino-laryngologie, d'[3]Endocrinologie, Hôpital de Bicêtre, Assistance Publique-Hôpitaux de Paris, Université Paris Sud, Le Kremlin-Bicêtre, France. [4] Department of Pharmaceutical Sciences, University of Antwerpen, Wilrijk. [5]Centre de Recherche Clinique, Centre Hospitalier Régional de Meaux, France. [6]Institut National de la Santé et de la Recherche Médicale, U693 Hôpital de Bicêtre, France. [7]Institut National de la Santé et de la Recherche Médicale, U894, Université ParisV Descartes, Paris, France.

Running head: Hyoid muscle performance and growth hormone

Corresponding author: Y. Lecarpentier, MD, PhD, Service de Physiologie, Hôpital de Bicêtre, Assistance Publique-Hôpitaux de Paris, 94275, le Kremlin-Bicêtre, FRANCE.

TEL: (331) 45 21 36 62

FAX: (331) 45 21 37 78

Email address; yves.lecarpentier@bct.aphp.fr

Copyright 2009 by the European Respiratory Society.

ABSTRACT: *In vitro* isotonic and isometric mechanical properties of the sternohyoid (SH) muscle, an upper airway dilator muscle, were studied in rats with a growth hormone-secreting tumour (GH; n = 10). The effects of muscle fatigue were also studied.

Stress and shortening were measured in muscles contracting from zero load up to isometric load under tetanic conditions. Isometric stress and maximum unloaded shortening velocity were determined and compared with values obtained from control rats (C; n = 10). Crossbridge (CB) kinetics and energetics and mechanical efficiency were calculated from Andrew F. Huxley's equations.

Compared with C, isometric stress, mechanical efficiency, CB number and CB single force were lower in GH. Probability of CB being in the power stroke configuration was lower in GH than in C. Muscle fatigue significantly impaired maximal muscle efficiency and CB single force in GH but not in C.

In conclusion, mechanical and energetic properties of the sternohyoid muscle and CB properties were worse in GH than in C. This may partly account for impairment of the upper airway dilator muscle function and the increased occurrence of obstructive sleep apnoea in acromegaly.

Key words: growth hormone, sternohyoid muscle, mechanics, myosin, fatigue, sleep apnoea syndrome

Upper airway dilator muscles exhibit phasic activity during inspiration (1,2). In synergy with the diaphragm, these muscles contribute to upper airway patency during breathing in awake and sleeping subjects (3). The negative pressure generated in the upper airways by diaphragm contraction is one of the most important factors involved in the stimulation of the pharyngeal dilator muscles, which promote opening of the upper airways during inspiration (3-5). The activity of pharyngeal muscles has also been studied in sleep apnoea syndrome, in which repeated occlusion of the upper airways occurs during sleep. Pharyngeal occlusions seem to be associated with a relative decline in activity of upper airway dilator muscles (3,6). The presence of enlarged pharyngeal muscles associated with weakness in these muscles is a well-recognized clinical observation in patients with acromegaly (7). Administration of growth hormone to animals produces an increase in muscle bulk (8). However during growth hormone hypersecretion syndrome, the contractile function of hypertrophied muscle has been shown to be decreased (9-11). Changes in mechanical properties of pharyngeal muscles may thus have important pathophysiological implications in the development of sleep apnoea syndrome, which has been shown to be prevalent in acromegaly (12,13).

The aim of the present study was to determine the isotonic and isometric mechanical properties of the sternohyoid muscle (SH), a pharyngeal dilator muscle, in rats with a growth hormone-secreting tumour. As diaphragm contractility has been previously shown to be impaired in a similar model of rat with a growth hormone-secreting tumour (11), we hypothesized that mechanical performance of SH muscle may also be decreased. In striated muscle, muscle performance is determined both by the number and the single force of crossbridges (CB) which represent molecular motors generating force and shortening. Using A. F. Huxley's equations (14), we determined CB single force, number and kinetics in SH muscle of rats with a growth hormone-secreting tumour.

Materials and methods

Animal model of rat with a growth hormone-secreting tumour

The investigation adhered to the APS's Guiding Principles in the Care and Use of Animals, to the National Institute of Health Guide for Care and Use of Laboratory Animals and was allowed by the Animal Ethics Committee of the French Institut National de la Santé et de la Recherche Médicale. All efforts were made to minimize pain and suffering and to reduce the number of animals used. Growth hormone-hypersecreting cells (GC) were cultured in Ham's F10 medium supplemented with 15% horse serum and 2.5% foetal calf serum (15-17) as previously described. Briefly, 12 x 10^6 cells were injected subcutaneously into the flank of 8-week old female Wistar-Furth rats (Charles River, France). Animals were housed in plastic containers, placed in a sound-proof room with controlled temperature (22–24 ° C) and illumination (12 h light, 12 h dark schedule with lights off at 19 h), fed ad libitum, and weighed weekly. SH muscle mechanical function was studied in isolated muscle strips from rats with a growth hormone-secreting tumour 12 weeks after GC injection (GH; n=10). SH muscle strips were also studied from control animals of the same age (C; n=10).

Hormonal immunoassays

After brief anaesthesia, blood samples were immediately collected into heparinized, chilled tubes, and the plasma stored at -20°C until assay. Plasma GH concentrations were evaluated by EIA as previously described (18). Values are reported in terms of rGH-RP2 with sensitivity of 0.6ng/ml. Intra- and inter-assay coefficients of variation were 4 and 14% respectively.

Mounting procedure

Animals were anesthetized with pentobarbital sodium (60 $mg.kg^{-1}$ intraperitoneally). SH muscle strips were removed via a median cervicotomy from the mandible to the manubrium and

after separation of the submaxillary glands. The suprahyoidian muscular attachments were cut, leaving the hyoid bone attached to the infrahyoid muscles. The hyoid bone was cut medially and then the two SH muscles were separated along the middle line as far as the inferior end of the muscles, requiring a sternotomy. A strip of SH muscle (2 mm width) was obtained by cutting one of the two SH muscles laterally. At the upper end of the strip, a piece of hyoid bone was left (hyoid end) and at the lower end a piece of sternum (sternum end). Each muscle strip was vertically suspended in a bath containing Krebs-Henseleit solution with the following composition (in mM): 118 NaCl, 4.7 KCl, 1.2 $MgSO_4$.7 H_2O, 1.1 KH_2PO_4, 24 $NaHCO_3$, 2.5 $CaCl_2$.6H_2O and 4.5 glucose. The solution was bubbled with 95% O_2/5% CO_2 and maintained at 26°C (pH 7.4). The sternum end of the SH muscle strip was held in a stationary clip at the bottom of the bath, and the hyoid end was held in a spring clip attached to an electromagnetic lever system. Muscles were stimulated by means of two platinum electrodes under tetanic conditions as follows: electrical stimulus 1 ms; stimulation frequency 100 Hz; train duration 200 ms; train frequency 5 trains.min^{-1}. At 26°C, the 100 Hz stimulation frequency yielded the maximum tetanic isometric active tension for the SH pharyngeal muscle. Experiments were carried out at the initial resting length (Lo) corresponding to the apex of the active tension versus initial length curve. At the end of the study, the cross-sectional area (in mm^2) was calculated from the ratio of fresh muscle weight to muscle length at Lo, assuming a muscle density of 1.06 g.mL^{-1}.

The electromagnetic lever system

The lever system was used to perform several tasks: to impose a well-determined preload and afterload on the muscle, to measure force exerted on the muscle and to measure length changes in the muscle (19). Force generation was based on the electromagnetic principle: a 30 mm-long lever was attached to a coil carrying a constant current. The coil was arranged in a constant magnetic field and a well-determined torque developed. Hence, a precision current source determined the force at the tip of the lever. This force could be set by decade switches in calibrated steps of 100, 10, 1 and 0.1 mN, up to a total of 140 mN. The error of the measured force was <

0.1%. The equivalent moving mass of the whole system was 155 mg and its compliance was 0.25 $\mu m.mN^{-1}$.

The displacement of the lever was measured by means of an opto-electronic transducer. A small diaphragm on the lever modulated the light from a tiny IR-LED falling on a photodiode with a daylight filter that blocked visible light but allowed near-IR radiation to pass. The photodiode current was converted to a voltage and filtered with an active third-order low pass filter (fc = 150 c/s) with optimal step response. The resulting length range was 5 mm at a full-scale output voltage of 10 V (error 1%) with a noise floor < 2.5µm p-p.

Force carried by the muscle preparation was measured with unilateral feedback techniques: the displacement signal was continuously compared to a reference voltage, corresponding to the stop position of the lever, and hence the resting length of the muscle. The servo loop kept the lever at this stop position as long as the muscle developed a force smaller than the total imposed load. However, if the muscle was stimulated and developed more force than this total load, the feedback became inactive, resulting in the muscle carrying this load during its isotonic contraction – relaxation cycle. The lever behaved as if a mechanical stop was guarding it against stretching the muscle beyond its resting length. The force signal filter had the same characteristics as above, eliminating a time skew between the force and displacement signal. Maximum range was 140 mN (20mN/V), with a noise floor < 0.05 mN.

All analyses were based on digital recordings obtained from a data acquisition system connected to a computer. Two signals, force and length, were recorded. Although data could be loaded in an Excel worksheet, a custom-made program was written to determine the most common muscle parameters automatically. It also calculated the first derivative of both channels to obtain the velocity of shortening and the rate of change of force.

Mechanical analysis, CB kinetics and energetics

The mechanical parameters of the muscle strips were calculated from two contractions at Lo and recorded in tetanus mode. The first contraction was abruptly clamped to zero-load 3ms after the

onset of the electrical stimulus. The second contraction was fully isometric. The following mechanical indices were used: maximum unloaded shortening velocity of contraction 1 (Vmax) and total force was the peak isometric force of contraction 2 (Fo). Velocity was expressed in $Lo.s^{-1}$, force (F) was normalized per muscle cross-sectional area (mm^2) of the SH muscle strip. i.e., stress (P) in $mN.mm^{-2}$ and time in s.

The hyperbolic stress-velocity (P -V) relationship was derived from the peak velocity (V) of 7 to 10 isotonic afterloaded contractions, plotted against the isotonic load level normalized per cross-sectional area (P), by successive load increments, from zero-load up to the isometric stress (Po). The P -V relationship was fitted according to A. Hill's equation (P+ a) (V+ b) = [Po+ a]b where - a and - b are the asymptotes of the hyperbola (20). For each SH muscle strip, the P -V relationship was accurately fitted by a hyperbola (each $r > 0.98$). The G curvature of Hill's hyperbola is equal to Po / a = Vmax / b (20,21).

A.F. Huxley' s equations (14) were used to calculate the maximum turnover rate of myosin ATPase under isometric conditions (kcat in s^{-1}), the elementary force per single CB interaction (π, in pN) and the number of active CBs per cross-sectional area (N) (22,23) (see the Appendix). Huxley's equations were also used to calculate CB kinetics (Fig.1), i.e., constants of CB attachment (f1 in s^{-1}) and detachment (g1 and g2 in s^{-1}), mean CB velocity during the power stroke and duration of the power stroke (vo in $\mu m.\ s^{-1}$ and ts in ms, respectively), the total duration of the CB cycle under isometric conditions (tc in ms), and peak efficiency (Effmax). Probabilities of three steps of the CB cycle, i.e., the detachment step (PD1), the attachment step (PA1), and the power stroke step (PA2) were also calculated (Fig.1) (see the Appendix).

Fatigue protocol

Muscle fatigue was induced by repeatedly stimulating each strip by means of 75 $trains.min^{-1}$ of 200-ms duration at a frequency of 100 Hz under isometric conditions. Total force was monitored and was found to decrease progressively. Stimulation continued until the muscle was fatigued to the point where it generated about 50% of baseline total force. Then mechanical parameters were

determined in tetanic mode using similar methods to those used before fatigue.

Statistical analysis

Data are expressed as means ± SEM. Controls were compared to GH using Student's unpaired t-test after ANOVA; p-values < 0.05 were required to rule out the null hypothesis. Linear regression was based on the least squares method. The asymptotes -a and -b of Hill's hyperbola were calculated by linear regression and the least squares method.

Results

Effects of tumour growth on body weight and plasma hormone levels

At the time of sacrifice, the mean body weight of GH was significantly higher than in C. In GH, the mean weight of the tumour was 13.2 ± 1.8 g at the time of the study, i.e., 12 weeks after GC injection. Growth hormone plasma levels were markedly higher in GH hypersecreting tumour-rats than in control rats (Table 1). The length of SH muscle did not differ significantly between the two groups.

Mechanics

Total stress (Po), total number of active crossbridges per mm^2 (N) and the single force of crossbridges (π) were significantly lower in GH than in C (Fig. 2). Vmax did not differ between the two groups (Fig. 2). The economy of contraction was worse in GH than in C as reflected by the significant decrease in peak muscle efficiency (Effmax) and G curvature (Table 1) (Fig. 3). The asymptote – a of the P -V hyperbola was significantly lower in GH than in C (Table 1), although the contrary was observed for the asymptote – b. The maintenance heat under isometric conditions (ab) did not differ between the two groups (Table 1).

Crossbridge kinetics and energetics

Constants of attachment (f1) and detachment (g1) were significantly higher in GH than in C (Table 1). However, g2, the detachment constant after the step size, did not differ between the two groups (Table 1). The maximum turnover of myosin ATPase (kcat) was also significantly higher in GH (Fig. 3). Both the duration of the power stroke step (ts) and the total duration of the crossbridge cycle under isometric conditions (tc) were significantly shorter in GH than in C (Fig. 3). Probabilities PD1 and PA1 were significantly higher in GH than in C (Fig. 4). Probability PA2 did not differ between the groups (Fig.4). Mean CB velocity during the stroke (vo) was significantly higher in GH than in C (Fig. 4).

Effects of fatigue

In both groups, muscles were fatigued to a similar extent (~ 50 % of Po) (Table 2). Vmax was significantly reduced in C ($p < 0.05$) whereas the decrease of Vmax in GH was not significant. Fatigue impaired the mechanics and energetics of both GH and C. Indeed, fatigue impaired the myothermal economy of contraction more in the GH group than in C, as indicated by the significant decrease in G curvature of the P-V relationship, Effmax and CB single force (Table 2).

Relationships between parameters

In the study groups as a whole, there was a direct linear relationship between the peak isometric stress (Po) and the number of active crossbridges (N) (fig. 5). A linear relationship was also found between kcat and vo (Fig. 5). No relationship existed between Po and π, the elementary force per single crossbridge. A curvilinear relationship was demonstrated between π and the G curvature (Fig. 5).

Discussion

We demonstrated that there were intrinsic alterations in the sternohyoid muscle mechanical performance in rats with a growth hormone-secreting tumour. The fall in total tension was

attributed to the decline in both the number and unitary force of CB myosin molecular motors. Moreover, muscle fatigue significantly impaired CB single force and muscle efficiency in GH, but not in C (Table 2). This may be important as upper airway dilator muscles have a respiratory function. They participate in preventing upper airway collapse when intrapharyngeal pressure becomes negative during inspiration. The pharynx is the only part of the large airways that lacks rigid support since its anterior wall is surrounded only by soft tissue (24). During sleep or unconsciousness, striated muscle tone is decreased, which reduces the muscular support of the pharyngeal area (25). This contributes to passive prolapse of the tongue and the soft palate and consequently favours obstruction of airflow (26). This mechanism is aggravated if pharyngeal mechanical performance is impaired (27). Failure of upper airway dilator muscles to maintain pharyngeal patency during sleep plays a role in the development of obstructive sleep apnoea. The ability to generate stress *in vitro* may differ from the ability to generate force *in vivo* and therefore the ability to create outer wall stress on the upper airways may not be changed. However, sleep apnoea syndrome is known to occur in clinical conditions involving pharyngeal neuromuscular dysfunction (27). Thus, a high prevalence of sleep apnoea has been reported in Charcot-Marie-Tooth disease and the severity of the sleep apnoea syndrome has been found to correlate with the severity of changes in motor nerve conduction. This suggests that neurogenic upper airway myopathy may contribute to sleep apnoea syndrome (28). Moreover, oculopharyngeal muscular dystrophy, which selectively affects the extraocular and pharyngeal muscles, has been reported to be associated with sleep apnoea syndrome in the absence of obesity or abnormal upper airway morphology (29). Thus, a myopathy can be associated with upper airway collapse which occurs uniquely during sleep and results in sleep apnoea syndrome. These studies show that upper airway myopathies may induce contractile dysfunction and sleep apnoea syndrome.

Myopathy in growth hormone hypersecretion syndrome

Greenbaum and Young found a general hypertrophy in various muscles in rats treated with pituitary extracts (8). Bigland and Jehring showed that tetanic isometric tension of hypertrophied

quadriceps was decreased in rats treated with growth hormone (9). In growth hormone-secreting Wistar-Furth rats, it has been found that the size of type I muscle fibres was increased to the greatest extent whereas type IIA fibres were unaffected (30).

Histological and histochemical studies have been performed on muscle biopsies in acromegalic patients. Mastaglia has described several abnormalities, namely isolated fibre necrosis or vacuolar degeneration, increased numbers of internal nuclei, high glycogen content, and either hypertrophy of type I and type II fibres or atrophy of both fibre types; and using electron microscopy also found large amounts of lipofuscin pigment in many fibres while some fibres had large sarcolemmal nuclei with prominent nucleoli and a prominent Golgi apparatus (31). Nagulesparen et al. (7) have described hypertrophy of type I muscle fibres, and atrophy of type II fibres. In other studies performed on acromegalic patients, histopathological analyses of skeletal muscle have shown sclerotic lesions, hypertrophic fibres, fibre degeneration, calcifications, altered mitochondria (elongation, matrical pallor, and cristae abnormalities), infiltration of glycogen granules, inclusion bodies, excess lipofuscin pigment and myofilament loss, and vesicular dilatations (32-34). Histological abnormalities can partly explain muscle weakness in patients with growth hormone hypersecretion. This cellular damage may also partly explain the decrease in CB density per CSA observed in our study (Fig.2c).

Upper airway dilator muscles have been shown to be faster and less resistant to fatigue than the diaphragm (35,36). In the rat, the myosin fibre type composition of the sternohyoid muscle is: 5% type I, 28% type IIa and 67% type IIb. That of the diaphragm is: 42% type I, 31% type IIa and 27% type IIb (37). The diaphragm, with a high type I fibre percentage, appears to be better adapted than the sternohyoid muscle to continuously overcoming elastic and resistive loads during breathing.

Crossbridge modifications in rats with a growth hormone-secreting tumour

The precise cellular and molecular effects of the growth hormone on striated muscles of the growth hormone-secreting tumour rat model used in the present study appear to be complex and

dependent on the type of sarcomeric muscle. Thus, total isometric tension and the G curvature of the P-V relationship have been found to be increased in heart muscle (16), contrary to observations in diaphragm (11) and sternohyoid muscles (Table 1 and Fig.2). Where CBs are concerned, changes in the kinetics of attachment and detachment (Table 1) (Fig.1) induced an increase in probabilities of states A1 and D1 in GH (Fig.4). Conversely, the probability of state A2, the power stroke step of the CB cycle, did not change. Together with the decrease in CB number and CB single force, this partly explained the decrease in contractile performance in GH (Fig.2). In diaphragm muscle of the same animal model, only the CB number has been found to be decreased, the CB single force remaining similar to controls (11). This shows that deleterious effects of massive growth hormone hypersecretion on CB mechanics and energetics were more marked in sternohyoid muscle than in diaphragm(38). This is corroborated by the decreased muscle efficiency observed in the sternohyoid muscle but not in the diaphragm (38). Differences in the fibre type composition between the two muscles may partly explain these results. Both the CB velocity and kcat were decreased in GH as compared with C, but remained linearly related (Fig.5). Moreover, fatigue in rat sternohyoid muscle has been found to induce unfavourable mechanical behaviour (38). However in the present study, the maximum unloaded shortening velocity (Vmax) was not modified in GH (Fig.2), due to the absence of change in the detachment constant g2 (Table 1) (14). Similar behaviour has been previously observed in heart muscle in the same GH rat model (16). The decrease in G curvature of the force-velocity relationship paralleled the decrease in CB single force according to a curvilinear relationship inherent to A.F. Huxley's equations (Table 1 and Fig.5) (14,23).

Effects of fatigue

It has been previously shown that effects of fatigue for a given species depend on the muscle concerned (38) and for a given muscle depend on the studied species. In rat diaphragm muscle, fatigue induces an increase in both the G curvature and muscle efficiency, although the contrary was observed in rat sternohyoid muscle. Differences in fibre type composition may partly explain these observations, with about 90% of fast type II fibres in rat SH and with a mixed fibre muscle

composition in rat diaphragm muscle (36,37,39)**.** In the present study, fatigue impaired the economy of muscle contraction and CB single force in GH although they were not significant in C (Table.2). Fatigue exacerbated the decrease in sternohyoid muscle efficiency and CB single force, already observed in baseline GH as compared to baseline C. Excessive fatigue and sensitivity to fatigue of the sternohyoid muscle may lead to increased pharyngeal resistance, inducing a vicious circle with aggravation of fatigue and failure of pharyngeal dilator muscle function.

Limitations

The results pertain strictly to the animal species and experimental conditions used. Mechanics and energetics of myosin crossbridges in human sternohyoid muscle probably differ from those of rat sternohyoid muscle. Moreover, the levels of plasma growth hormone were dramatically higher in rats with a growth hormone-secreting tumour than those observed in human acromegaly.

Clinical Relevance

It is important to consider the function of the pharyngeal dilator muscles during growth hormone hypersecretion in humans. Sleep apnoea syndrome is prevalent in acromegaly (13) and has been shown to increase morbidity and mortality (12). Indeed, death due to respiratory disease has been found to be three times more likely in acromegaly (40). Several respiratory disorders have been previously described in patients with growth hormone hypersecretion syndrome (41). Pneumomegaly has been attributed to an increase in the size or number of alveoli. Growth hormone hypersecretion increases upper airway resistance and this has been thought to aggravate respiratory disorders due to an increase in the work of breathing, which may lead to diaphragm fatigue and/or weakness. In humans, narrowing of the upper airways with the development of airflow obstruction has many etiological factors in acromegaly**:** hypertrophy of soft tissues of the tongue, pharynx and larynx, structural modification of facial bones and notably a development and rotation of the mandibula with retroposition of the tongue. An increase in upper airway resistance induces an

increase in the work of the pharyngeal dilators in order to open the airways during inspiration. In association with intrinsic alterations of muscular cells due to growth hormone hypersecretion, this may partly account for the impairment of pharyngeal and diaphragm strength (1), which promotes obstructive sleep apnoea. Finally, growth hormone hypersecretion results in generalized weakness and wasting of skeletal muscles.

Conclusion

Growth hormone hypersecretion in rats induced major intrinsic impairment of the mechanical performance of the sternohyoid muscle, one of the pharyngeal dilator muscles. The mechanical and energetic profile of the sternohyoid muscle was characterized by a significant fall in both crossbridge number and crossbridge single force, decreased muscle efficiency and alterations in crossbridge kinetics.

Appendix

CB Characteristics

The rate of total energy release (E_{Hux}) and the isotonic tension (P_{Hux}) as a function of muscle velocity (V) are given by A. F. Huxley's equations (14):

$$E_{Hux} = Ne\frac{h}{2l}\frac{f_1}{f_1+g_1}\left\{g_1+f_1\frac{V}{\phi}\left(1-e^{-\frac{\phi}{V}}\right)\right\}$$

$$P_{Hux} = N\frac{sw}{2l}\cdot\frac{f_1}{f_1+g_1}\left[1-\frac{V}{\phi}\left(1-e^{\frac{\phi}{V}}\right)\left(1+\frac{1}{2}\left(\frac{f_{1+}g_1}{g_2}\right)^2\frac{V}{\phi}\right)\right]$$

where N is the cycling CB number per mm^2 at peak isometric tension; s is the resting optimal sarcomere length (s = 2.2 μm); f_1 is the peak value of the rate constant for CB attachment; and g_1 and g_2 are the peak values of the rate constants for CB detachment. The tilt of the myosin head relative to actin varies from 0 to h; f_1 and g_1 correspond to a tilt = 0, and g_2 corresponds to a tilt > h; $\phi = (f_1 + g_1)\, h / s = b$.

w i s the maximum mechanical work of a single CB (w / e = 0.75) (14). According to A.F. Huxley's theory (14) one ATP molecule is split per CB cycle. The standard free energy $\Delta G°'_{ATP}$, e is equal to 5.1×10^{-20} J (21); $\Delta G°'_{ATP}$ has been found to be -32 kJ /mol at pH 7.0 and 37°C (42).

The parameter l is the distance between successive actin sites with which any one myosin site can combine. In Huxley's work (14), the calculated estimate of l was found to be 15.3 nm. This value corresponds approximately to the meridional spot at 14.3 nm determined by means of X-ray diffraction and arising from the helical arrangement of crossbridges on the thick filament (43). This is of the same order of magnitude as the distance corresponding to three successive G-actin monomers. For a given actin filament, the distance l between two actin sites with which a myosin site can combine was chosen to be equal to 14.3 nm. The molecular step size h is defined by the translocation distance of the actin filament per ATP hydrolysis, produced by the swing of the myosin head (44). A.F. Huxley's equations assume that l is much greater than h. The value of h was chosen to be equal to 5nm, a value supported by optical tweezer experiments on muscle myosin II (45).

Calculations of f_1, g_1 and g_2 are given by the following equations (23):

$$G = f_1 / g_1 \; ; \qquad g_1 = \frac{swb}{ehG} \; ; \qquad g_2 = \frac{sV_{max}}{h}$$

$$kcat = (h/2l) \times [(f_1 g_1) / (f_1 + g_1)] \text{ and } \pi = (w/l) \times [(f_1) / (f_1 + g_1)]$$

The number of active CBs (N) is equal to the ratio of the peak isometric tension and the elementary CB force (π).

The rate of mechanical work (W_M) is given by the equation: $W_M = P_{Hux} . V$

At any given load level, the mechanical efficiency (Eff) of the muscle is defined as the ratio of W_M to E_{Hux} i.e., $Eff = W_M / E_{Hux}$ and Eff_{max} is the peak value of Eff.

Acknowledgments: Pierre Attal was Associate Professor from 1 September 2005 to 31 August 2007, University Paris Sud.

References

1. Sauerland EK, Harper RM. The human tongue during sleep: electromyographic activity of the genioglossus muscle. *Exp Neurol* 1976;51:160-70.
2. Sherrey JH, Pollard MJ, Megirian D. Respiratory functions of the inferior pharyngeal constrictor and sternohyoid muscles during sleep. *Exp Neurol* 1986;92:267-77.
3. Remmers JE, deGroot WJ, Sauerland EK, Anch AM. Pathogenesis of upper airway occlusion during sleep. *J Appl Physiol* 1978;44:931-8.
4. Mathew OP. Upper airway negative-pressure effects on respiratory activity of upper airway muscles. *J Appl Physiol* 1984;56:500-5.
5. Horner RL, Innes JA, Murphy K, Guz A. Evidence for reflex upper airway dilator muscle activation by sudden negative airway pressure in man. *J Physiol* 1991;436:15-29.
6. Fogel RB, Malhotra A, White DP. Sleep. 2: pathophysiology of obstructive sleep apnoea/hypopnoea syndrome. *Thorax* 2004;59:159-63.
7. Nagulesparen M, Trickey R, Davies MJ, Jenkins JS. Muscle changes in acromegaly. *Br Med J* 1976;2:914-5.
8. Greenbaum AL, Young FJ. Distribution of protein in the tissues of rats treated with anterior-pituitary growth-hormone. *Nature* 1950;165:521-522.
9. Bigland B, Jehring B. Muscle performance in rats, normal and treated with growth hormone. *J Physiol* 1952;116:129-36.
10. Wolf E, Wanke R, Schenck E, Hermanns W, Brem G. Effects of growth hormone overproduction on grip strength of transgenic mice. *Eur J Endocrinol* 1995;133:735-40.
11. Lecarpentier Y, Coirault C, Riou B, Chemla D, Mercadier JJ. Diaphragm strength and cross-bridge properties during chronic growth hormone hypersecretion. *Eur Respir J* 1999;13:1070-7.
12. Colao A, Ferone D, Marzullo P, Lombardi G. Systemic complications of acromegaly:

epidemiology, pathogenesis, and management. *Endocr Rev* 2004;25:102-52.

13. Davi MV, Carbonare LD, Giustina A, et al. Sleep apnoea syndrome is highly prevalent in acromegaly and only partially reversible after biochemical control of the disease. *Eur J Endocrinol* 2008;159:533-40.
14. Huxley AF. Muscle structure and theories of contraction. *Prog Biophys Biophys Chem* 1957;7:255-318.
15. Bertherat J, Timsit J, Bluet-Pajot MT, et al. Chronic growth hormone (GH) hypersecretion induces reciprocal and reversible changes in mRNA levels from hypothalamic GH-releasing hormone and somatostatin neurons in the rat. *J Clin Invest* 1993;91:1783-91.
16. Timsit J, Riou B, Bertherat J, et al. Effects of chronic growth hormone hypersecretion on intrinsic contractility, energetics, isomyosin pattern, and myosin adenosine triphosphatase activity of rat left ventricle. *J Clin Invest* 1990;86:507-15.
17. Kamenicky P, Viengchareun S, Blanchard A, et al. Epithelial sodium channel is a key mediator of growth hormone-induced sodium retention in acromegaly. *Endocrinology* 2008;149:3294-305.
18. Ezan E, Laplante E, Bluet-Pajot MT, et al. An enzyme immunoassay for rat growth hormone: validation and application to the determination of plasma levels and in vitro release. *J Immunoassay* 1997;18:335-56.
19. Sys SU, De Keulenaer GW, Brutsaert DL. Physiopharmacological evaluation of myocardial performance: how to study modulation by cardiac endothelium and related humoral factors? *Cardiovasc Res* 1998;39:136-47.
20. Hill AV. The heat of shortening and the dynamic constants of muscle. Proc. R. Soc. Lond. Biol. Sci 1938;126:136-195.
21. Woledge RC, Curtin AN, Homsher E. Energetic Aspects of Muscle Contraction. London: Academic Press, 1985.
22. Coirault C, Lambert F, Joseph T, Blanc FX, Chemla D, Lecarpentier Y. Developmental changes in crossbridge properties and myosin isoforms in hamster diaphragm. *Am J Respir*

Crit Care Med 1997;156:959-67.

23. Lecarpentier Y, Chemla D, Blanc FX, et al. Mechanics, energetics, and crossbridge kinetics of rabbit diaphragm during congestive heart failure. *Faseb J* 1998;12:981-9.

24. Eckert DJ, Malhotra A. Pathophysiology of adult obstructive sleep apnea. *Proc Am Thorac Soc* 2008;5:144-53.

25. Worsnop C, Kay A, Pierce R, Kim Y, Trinder J. Activity of respiratory pump and upper airway muscles during sleep onset. *J Appl Physiol* 1998;85:908-20.

26. Wheatley JR, Tangel DJ, Mezzanotte WS, White DP. Influence of sleep on response to negative airway pressure of tensor palatini muscle and retropalatal airway. *J Appl Physiol* 1993;75:2117-24.

27. Kimoff RJ. Upperairway myopathy is important in the pathophysiology of obstructive sleep apnea. *J Clin Sleep Med* 2007;3:567-9.

28. Dematteis M, Pepin JL, Jeanmart M, Deschaux C, Labarre-Vila A, Levy P. Charcot-Marie-Tooth disease and sleep apnoea syndrome: a family study. *Lancet* 2001;357:267-72.

29. Dedrick DL, Brown LK. Obstructive sleep apnea syndrome complicating oculopharyngeal muscular dystrophy. *Chest* 2004;125:334-6.

30. Prysor-Jones RA, Jenkins JS. Effect of excessive secretion of growth hormone on tissues of the rat, with particular reference to the heart and skeletal muscle. *J Endocrinol* 1980;85:75-82.

31. Mastaglia FL. Pathological changes in skeletal muscle in acromegaly. *Acta Neuropathol* 1973;24:273-86.

32. Cheah JS, Chua SP, Ho CL. Ultrastructure of the skeletal muscles in acromegaly--before and after hypophysectomy. *Am J Med Sci* 1975;269:183-7.

33. Pickett JB, Layzer RB, Levin SR, Scheider V, Campbell MJ, Sumner AJ. Neuromuscular complications of acromegaly. *Neurology* 1975;25:638-45.

34. Khaleeli AA, Levy RD, Edwards RH, et al. The neuromuscular features of acromegaly: a clinical and pathological study. *J Neurol Neurosurg Psychiatry* 1984;47:1009-15.

35. van Lunteren E, Salomone RJ, Manubay P, Supinski GS, Dick TE. Contractile and endurance properties of geniohyoid and diaphragm muscles. *J Appl Physiol* 1990;69:1992-7.

36. Dick TE, van Lunteren E. Fiber subtype distribution of pharyngeal dilator muscles and diaphragm in the cat. *J Appl Physiol* 1990;68:2237-40.

37. Bracher A, Coleman R, Schnall R, Oliven A. Histochemical properties of upper airway muscles: comparison of dilator and nondilator muscles. *Eur Respir J* 1997;10:990-3.

38. Attal P, Coirault C, Chemla D, et al. Isotonic mechanics of a pharyngeal dilator muscle and diaphragm in the rat before and after fatigue. *Eur Respir J* 2000;15:308-13.

39. Petrof BJ, Kelly AM, Rubinstein NA, Pack AI. Effect of hypothyroidism on myosin heavy chain expression in rat pharyngeal dilator muscles. *J Appl Physiol* 1992;73:179-87.

40. Hochban W, Ehlenz K, Conradt R, Brandenburg U. Obstructive sleep apnoea in acromegaly: the role of craniofacial changes. *Eur Respir J* 1999;14:196-202.

41. Trotman-Dickenson B, Weetman AP, Hughes JM. Upper airflow obstruction and pulmonary function in acromegaly: relationship to disease activity. *Q J Med* 1991;79:527-38.

42. Veech RL, Lawson JW, Cornell NW, Krebs HA. Cytosolic phosphorylation potential. *J Biol Chem* 1979;254:6538-47.

43. Squire JM. The Structural Basis of Muscular Contraction. New York: Plenum Press, 1981.

44. Huxley HE. The mechanism of muscular contraction. *Science* 1969;164:1356-65.

45. Molloy JE, Burns JE, Kendrick-Jones J, Tregear RT, White DC. Movement and force produced by a single myosin head. *Nature* 1995;378:209-12.

46. Eisenberg E, Hill TL, Chen Y. Cross-bridge model of muscle contraction. Quantitative analysis. *Biophys J* 1980;29:195-227.

Table 1. Effects of growth hormone secretion on body weight, plasma hormone levels, Hill's coefficients and CB kinetics.

	Control group	GH group
Body weight (g)	207 ± 3.7	437.4 ± 16.4 ($p<0.001$)
Muscle strip length (mm)	31.2 ± 2.3	31.3 ± 5.3 (NS)
GH plasma levels ($\mu g.L^{-1}$)	8.1 ± 4.3	6807 ± 3523 ($p<0.001$)
a ($mN.mm^{-2}$)	17.56 ± 6.8	10.72 ± 4.18 ($p<0.05$)
b ($Lo.s^{-1}$)	1.09 ± 0.37	1.52 ± 0.43 ($p<0.05$)
G	4.42 ± 1.39	3.23 ± 0.92 ($p<0.05$)
ab ($mN.mm^{-2}$. Lo. s^{-1})	19.9 ±12.6	16.4 ± 8.1 (NS)
f1 (s^{-1})	326 ± 110	456 ± 128 ($p<0.05$)
g1 (s^{-1})	87 ± 55	159 ± 80 ($p<0.05$)
g2 (s^{-1})	1828 ± 394	1820 ± 409 (NS)

Data are presented as mean ± SEM ; - a and - b are the asymptotes of the Hill hyperbola; G is the curvature of the hyperbola; f1 is the CB attachment constant; g1 and g2 are the CB detachment constant.

Table 2. Effects of fatigue on sternohyoid muscle in control and GH groups.

	Control group	GH group
Po	- 54 ± 5 *	- 46 ± 9 *
Vmax	- 21 ± 3 *	- 7 ± 2
G	- 18 ± 9	- 32 ± 7 *
Effmax	- 7 ± 4	- 16 ± 2 *
π	- 6 ± 4	- 13 ± 2 *

Data are presented as mean ± SEM of percentage changes induced by fatigue versus baseline. Po: total isometric stress; Vmax: maximum unloaded shortening velocity; G: curvature of Hill's hyperbola; Effmax: peak mechanical efficiency; π : CB single force. *:$p < 0.05$ fatigue versus baseline.

Legends of figures

Fig. 1. The ATP-ADP-Pi-actomyosin CB cycle. The CB cycle was subdivided into six different conformational states, with three detached states (D1, D2, and D3) and three attached states (A1, A2, and A3). Transition A3--> D1 was the ATP binding step; CB detachment occurred when ATP bound to the actin (A)-myosin (M) complex (AM) and the rate constant for detachment was g2; AM --> A + M. Transition D1--> D2 was the ATP hydrolysis; M + ATP --> M - ADP-Pi. Transition D2--> D3 was M - ADP-Pi --> M*-ADP-Pi, where M* is myosin in refractory state (46). Transition D3--> A1 was the attachment state: the myosin head (M*-ADP-Pi) weakly bound to A and the rate constant for attachment was f1; M - ADP-Pi + A --> AM-ADP-Pi. Transition A1 -->A2 was the power stroke, a strongly bound, high-force state which is triggered by Pi release: AM-ADP-Pi --> AM-ADP + Pi; ts was the duration of the power stroke. Transition A2 --> A3 was the release of the hydrolysis product ADP: AM - ADP --> AM + ADP; tc was the duration of the overall CB cycle and kcat = 1 / tc.

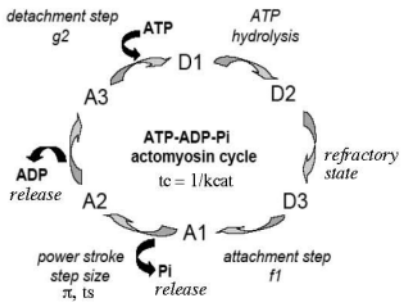

Fig. 2. A: isometric stress (Po); B: Maximum unloaded shortening velocity (Vmax); C: number (N) of active CBs per cross-sectional area; and D: the elementary force(π) per single CB. Data are presented as means ± SEM for C (white) and GH (grey). NS: non significant; *: $p < 0.05$; † : $p < 0.001$.

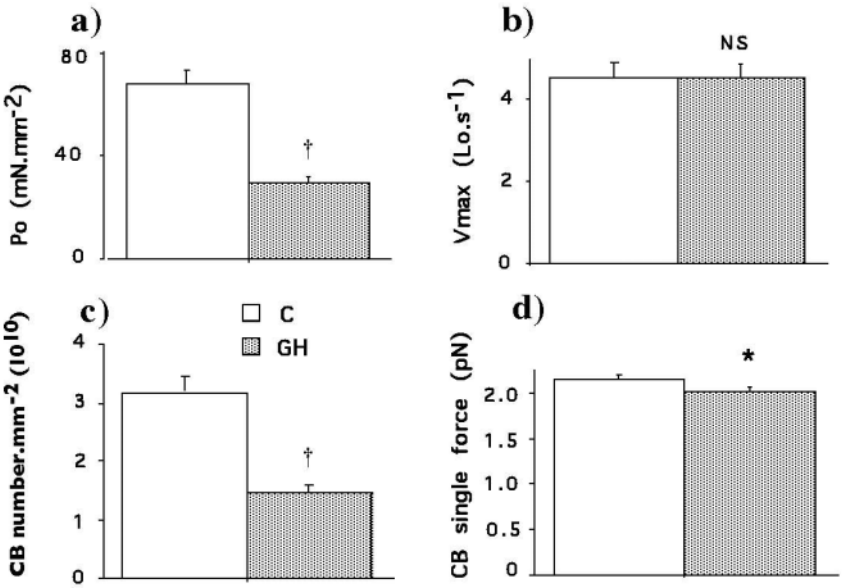

Fig.3. A: kcat; B: peak mechanical efficiency (Effmax); C: duration of the power stroke step (ts) and D: total duration of the CB cycle under isometric conditions (tc). Data are presented as means ± SEM for C (white) and GH (grey). NS: non significant; *: $p < 0.05$.

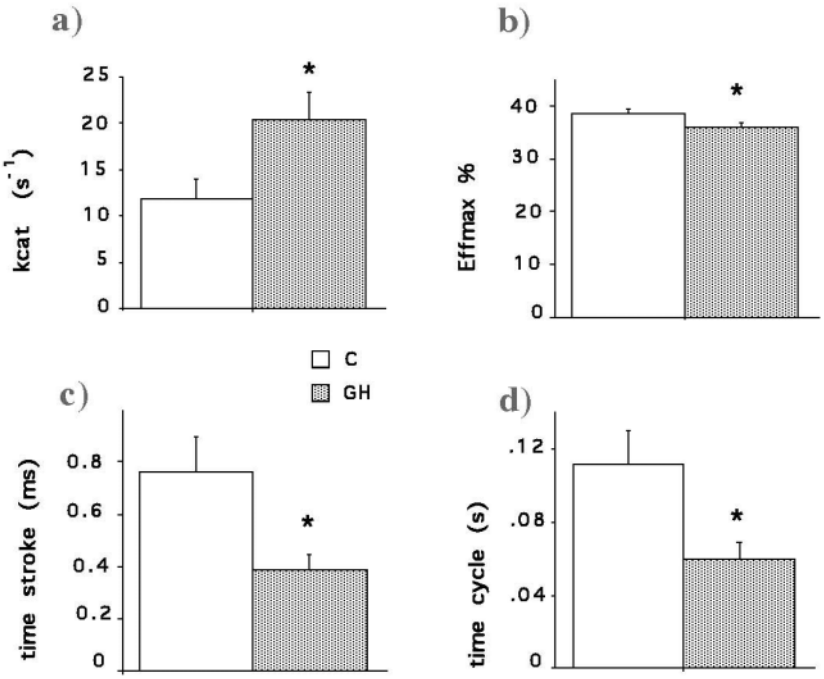

Fig.4. A: Probability of D1 state (PD1); B: Probability of A1 state (PA1); C: Probability of A2 state (PA2); and D: CB velocity during the stroke (vo). Data are presented as means ± SEM for C (white) and GH (grey). NS: non significant; *: $p < 0.05$.

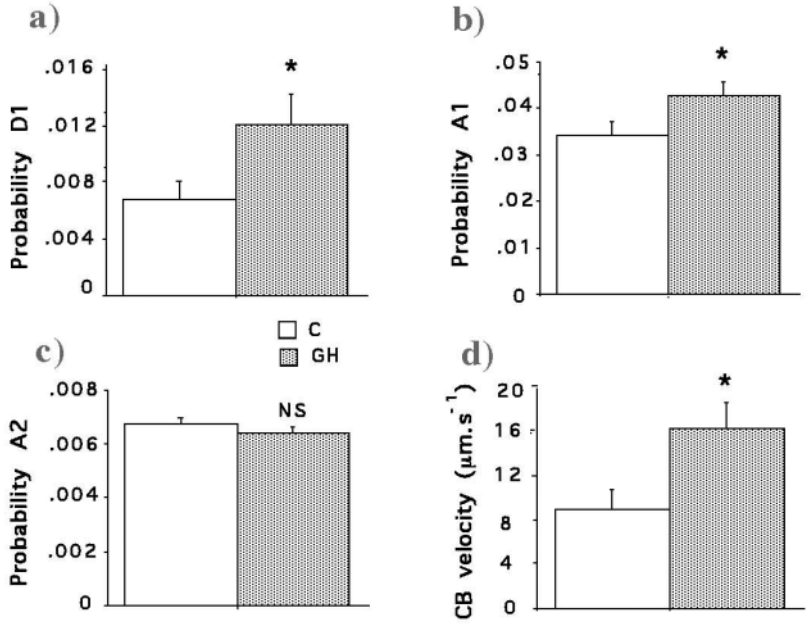

Fig.5. A: Linear relationship between isometric stress (Po) and active CB number per cross-sectional area (N) in C (r = 0.970) and GH (= 0.904); B: relationship between isometric stress (Po) and the elementary force (π) per single CB in C and GH; C: linear relationship between kcat and CB velocity during the stroke (vo) in C (r = 0.977) and GH (r = 0.853); D: curvilinear relationship between elementary force (π) per single CB and the G curvature in C and GH.

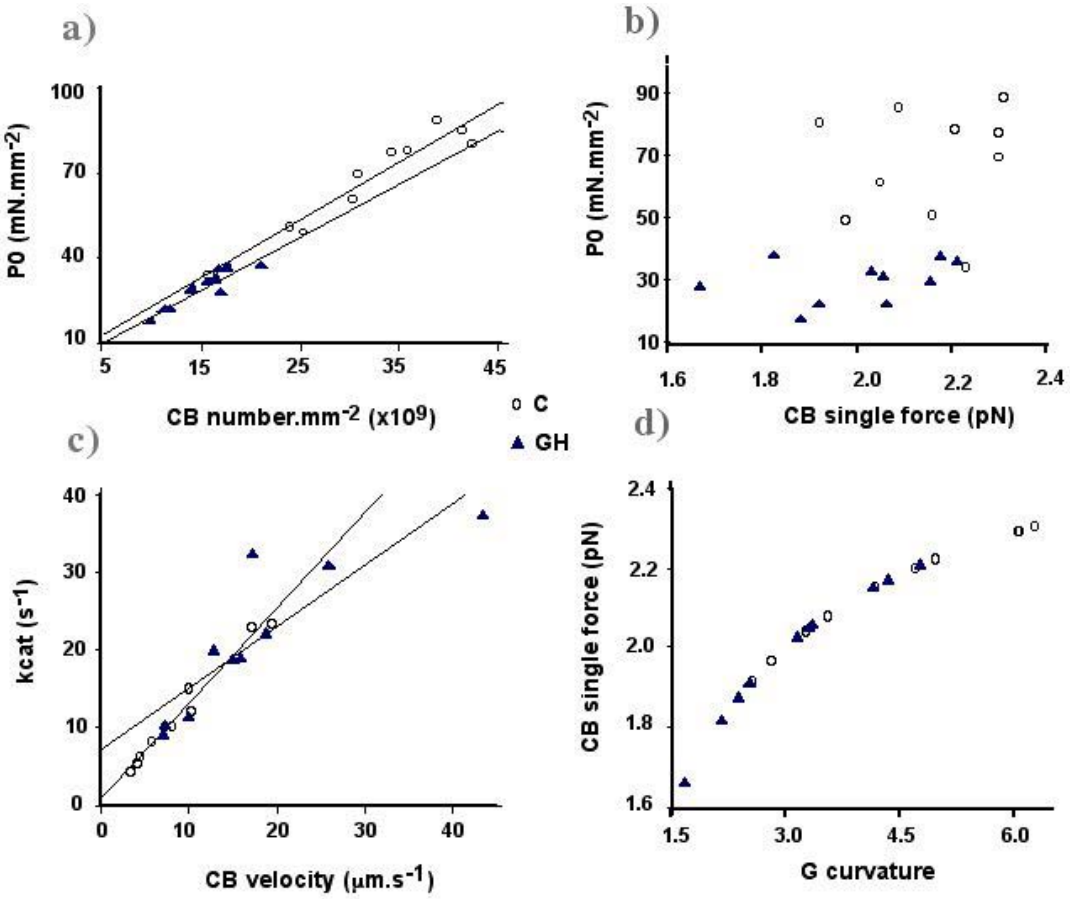
a)
b)
c)
d)
P0 (mN.mm-2)
CB number.mm-2 (x109)
C
GH
CB single force (pN)
kcat (s-1)
CB velocity (µm.s-1)
G curvature